FAST AND ACCURATE IRIS SEGMENTATION BASED ON LINEAR BASIS FUNCTION AND RANSAC

Kai Wang and Yuntao Qian

College of Computer Science, Zhejiang University, Hangzhou, China
zdwk223, ytqian@zju.edu.cn

ABSTRACT

Iris segmentation is a component of iris recognition system, and noncircular iris is hard to segment accurately. This paper presents an iris segmentation algorithm using linear basis function and RANSAC (Random SAmple Consensus) which iterately derives fine iris boundary curves from coarse iris boundary points. The algorithm consists of three steps. In step 1, coarse center and radius of iris are found using IDO (IntegroDifferential Operators); in step 2, coarse iris boundary points are located, and then a linear basis function model is constructed to derive coarse iris boundary curves from the boundary points; and in step 3, a RANSAC method is applied to refine the iris boundary curves. The proposed algorithm is tested on two datasets CASIA-Iris V3-Interval and IITD v1.0 and shows the effectiveness comparing with some popular algorithms.

Index Terms— Iris segmentation, Noncircular iris, IDO, Linear basis function, RANSAC

1. INTRODUCTION

Iris is the gray circular area around the pupil. Under the illumination of near-infrared light, iris is rich of texture, the texture is stable and unique for everyone, which makes it ideal as a biometric. Iris recognition system generally consists of four main modules [1]: image acquisition, iris segmentation, feature extraction, and matching. During iris segmentation, inner and outer boundaries of iris are found. Performances of the next steps, feature extraction and matching, strictly depend on result of iris segmentation, and segmentation errors will significantly increase the HD (Hamming Distance) between the iris images of a same eye [2]. Thus iris segmentation is a crucial component of iris recognition system.

Present iris segmentation algorithms can be grouped into two classes. The first class assumes that iris is circular or oval, such as IDO (IntegroDifferential Operators) [3], Hough Transform algorithm [4], and ellipse fitting algorithm [5]. The second class assumes that iris is noncircular, such as AC (Active Contours) [6], and GAC (Geodesic Active Contours) [7]. The second class seems to be more reasonable, since iris images captured in commercial iris recognition systems are always noncircular. Daugman discussed that the EER (Equal Error Rate) can be decreased by 90% by adapting AC instead of enforcing circular models on some irises from NIST ICE-1 iris database [6].

Algorithms based on circular iris assumption produce errors while segmenting irises with complex shapes, as is shown in Fig.2(b). However, we can use them to obtain coarse iris boundary points, then finding fine iris boundary is equal to the machine learning problem which derives function curves from data points.

In this paper we present an iris segmentation algorithm that deals with noncircular iris using linear basis function and RANSAC [8]. The algorithm contains three steps: step 1 finds the coarse iris center and radius by IDO; step 2 derives the iris boundary by a linear basis function model; step 3 refines the iris boundary by RANSAC. A great advantage of our algorithm is that it segments iris inner boundary accurately, while it is reported that the iris points nearer the inner boundary is more valuable than the other points [9].

The basis functions we choose in the linear basis function model are trigonometric functions, which are similar with Fourier Expansion, which was used for iris segmentation by Daugman [6]. As we know, the trigonometric functions may be the best basis functions we can find for iris segmentation.

2. THE COARSE CENTER AND RADIUS

The first step is to find the coarse iris center and radius of iris. Most of the present iris segmentation algorithms are capable for this job, we choose IDO in this article because it is proofed to be fast and accurate. IDO searches for the circle that has the biggest sum of normalized gradient differentiation:

$$\max_{(r,x,y)} \left| G_\sigma(r) * \frac{\partial}{\partial r} \oint_{r,x,y} \frac{I(x,y)}{2\pi r} ds \right| \qquad (1)$$

where (x, y) and r are center and radius of the circle searched respectively, I is the iris image, $G_\sigma(r)$ is a smoothing function, $*$ denotes convolution.

Fig.2(b) illustrates the located coarse circles.

This work was supported by the National Natural Science Foundation of China No.60872071

3. THE COARSE BOUNDARY CURVES

The second step of the algorithm is to derive the iris boundary curves from the coarse iris boundary points. This step consists of three substeps.

Firstly, the circular area of the upper $H/2$ and the lower $H/2$ of each circle is projected to a rectangle whose height is H and width is N, as is shown in Fig.1. The projection function is Eq.(2), where (x_c, y_c) is point on the circular, (i, h_i) is the according point on the rectangle. Fig.2(c, g) are illustrations of the projected rectangle.

$$\begin{cases} x_c = (r + h_i - \frac{H}{2})\cos(360\frac{i}{N}) \\ y_c = (r + h_i - \frac{H}{2})\sin(360\frac{i}{N}) \end{cases} \quad (2)$$

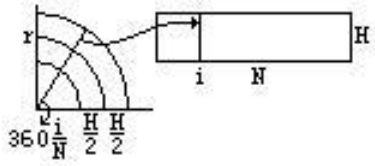

Fig. 1. Representation of the map from the circular area to the rectangle.

Secondly, for each column of the projected rectangle, the point with the largest difference is labeled as coarse iris boundary point. Fig.2(d, h) are illustrations. The points locate at the top or bottom of the rectangle are often errors result from occlusion by eyelids, eyelashes and specularities, the error points are simply deleted from our model. That is to say not all the boundary points on the rectangle are used. Let N_1 be the number of valid points, let (x_i, h_i) be the coordinates of the ith valid point on the rectangle, $i = 1, 2, , N_1$.

Thirdly, coarse iris boundary curves are derived from the coarse iris boundary points, which is a typical machine learning problem. To choose the machine learning model, three requirements need to be met. Firstly, irises have a variety of shapes such as round, oval, chestnut shaped, so the model must be flexible enough to fit these shapes; secondly, iris boundary is always influenced by occlusion by eyelids, eyelashes and specularities, which causes outliers or errors, so the model must be robust enough to deal with these outliers; thirdly, biometric systems have a high requirement of speed, so the model must be time economic. According to the first requirement, conical models are abandoned because they are not flexible enough. According to the third requirement, nonlinear models are rejected because they are always high of computational complexity and time-consuming. Finally, the linear basis function model [10] is chosen. Linear basis function model can fit any shape of curve by the careful selection of basis functions, its robustness can be adjusted by controlling the number of basis functions, and it is a linear model, which makes it very fast.

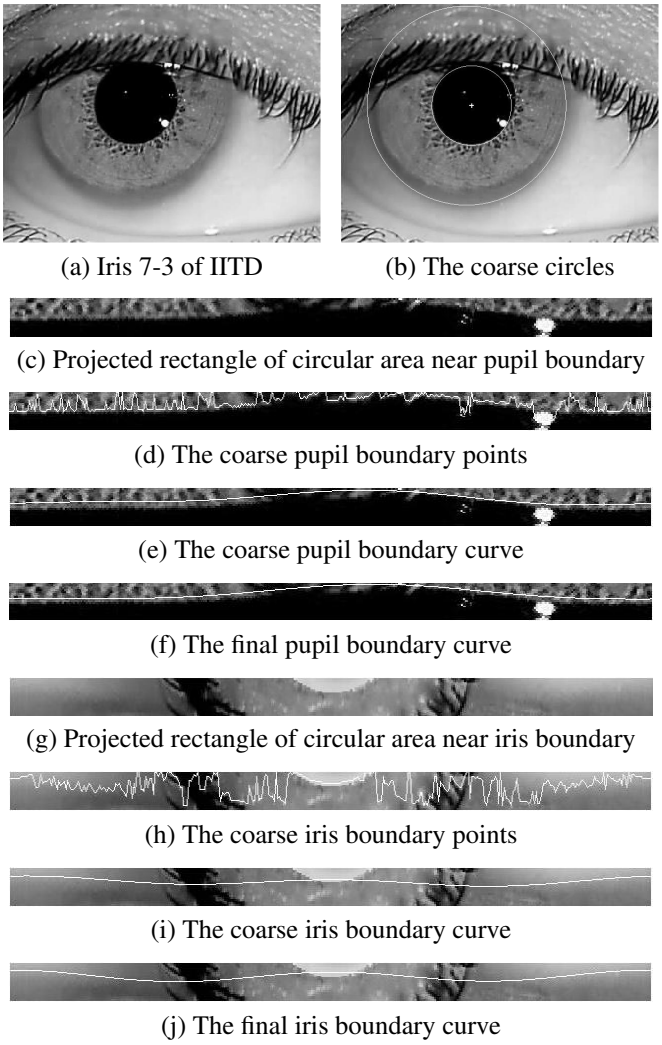

(a) Iris 7-3 of IITD (b) The coarse circles

(c) Projected rectangle of circular area near pupil boundary

(d) The coarse pupil boundary points

(e) The coarse pupil boundary curve

(f) The final pupil boundary curve

(g) Projected rectangle of circular area near iris boundary

(h) The coarse iris boundary points

(i) The coarse iris boundary curve

(j) The final iris boundary curve

Fig. 2. Illustration of the processes of the proposed method. The final segmentation result is shown in Fig.3.

The left most boundary point on the rectangle is adjacent with the right most boundary point, thus the boundary curve should have a period of N, which makes the trigonometric functions $(\cos(\frac{2\pi k}{N}), \sin(\frac{2\pi k}{N}))(k = 1, 2,)$ ideal as the basis functions. Their periods are $\frac{N}{k}$, which makes the left most boundary point naturally adjacent with the right most boundary point. On the other hand, these basis functions contain both odd functions and even functions, makes it capable to fit any shape of curve.

The bigger the number of basis functions, the irregular the boundary curves; the smaller, the smoother. Especially, when the number of focus functions is 0, the according boundary curves are circles. Experiments show that the model can fit iris shape accurately and can be robust enough to eliminate influences by occlusion in the same time, when the number of basis functions is set to 4. The according basis functions are:

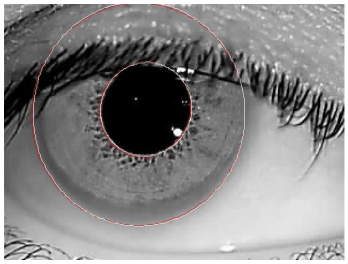

Fig. 3. The segment results of the proposed method. The white curves are the pupil and iris boundary curves before RANSAC. The red curves are the pupil and iris boundary curves after RANSAC.

$$\begin{cases} \phi_0(x) = 1 \\ \phi_1(x) = \cos\frac{2\pi x}{N} \\ \phi_2(x) = \sin\frac{2\pi x}{N} \\ \phi_3(x) = \cos\frac{4\pi x}{N} \\ \phi_4(x) = \sin\frac{4\pi x}{N} \end{cases} \tag{3}$$

ϕ_0 is dummy basis function that doesnot count. Boundary curve function in this linear basis function model is

$$y_i = w_0\phi_0(x_i)+w_1\phi_1(x_i)+w_2\phi_2(x_i)+w_3\phi_3(x_i)+w_4\phi_4(x_i) \tag{4}$$

or

$$y_i = \mathbf{w}^T\Phi(x_i) \tag{5}$$

where $i = 1, 2, ..., N_1$, $\mathbf{w} = (w_0, ..., w_4)^T$, $\Phi = (\phi_0, ..., \phi_4)^T$. According to the linear basis function model, we have

$$h_i = y_i + \varepsilon \tag{6}$$

where ε is supposed to be a zero mean Gaussian random variable. We can use maximum likelihood to determine $\mathbf{w}$. The maximization of the likelihood function under a conditional Gaussian random variable for a linear model is equivalent to minimize the sum-of-squares error function defined by

$$E_D(\mathbf{w}) = \frac{1}{2}\sum_{i=1}^{N_1}\{h_i - \mathbf{w}^T\Phi(x_i)\}^2 \tag{7}$$

The gradient of Eq.(7) takes the form

$$\nabla E_D(\mathbf{w}) = \sum_{i=1}^{N_1}(h_i - \mathbf{w}^T\Phi(x_i))\Phi(x_i)^T \tag{8}$$

Setting the gradient to zero gives

$$\sum_{i=1}^{N_1} h_i\Phi(x_i)^T - \mathbf{w}^T(\sum_{i=1}^{N_1}\Phi(x_i)\Phi(x_i)^T) = 0 \tag{9}$$

Solving the equation for $\mathbf{w}$ we obtain

$$\mathbf{w} = (\varphi^T\varphi)^{-1}\varphi^T\mathbf{t} \tag{10}$$

where

$$\varphi = \begin{bmatrix} \phi_0(x_1) & \phi_1(x_1) & \cdots & \phi_4(x_1) \\ \phi_0(x_2) & \phi_1(x_2) & \cdots & \phi_4(x_2) \\ \vdots & \vdots & \ddots & \vdots \\ \phi_0(x_{N_1}) & \phi_1(x_{N_1}) & \cdots & \phi_4(x_{N_1}) \end{bmatrix}$$

$$\mathbf{t} = [h_1, h_2, ..., h_{N_1}]^T$$

Fig.2(e, i) illustrate the boundary curves obtained by the linear basis function model.

The linear basis function processes very fast, cost only $0.1ms$ when N is set to 360, processed on a Xeon-Core computer (2.27GHz×4). Further more, when all the coarse boundary points are valid, the matrix is the same for all images, so it can be calculated offline.

4. THE FINE BOUNDARY CURVES

Linear basis function model can deal with outliers by controlling number of basis functions. However, linear basis function model assumes that error in Eq.6 is a zero mean Gaussian random variable, which doesnot hold when there are outliers. In order to obtain more accurate iris boundary, RANSAC is proposed to eliminate outliers. The RANSAC process contains these steps.

1. The linear basis function model is applied to all the valid boundary points whose number is N_1;

2. Calculate distance from each valid boundary point to the boundary curve obtained by the linear basis function model;

3. Set a threshold, if a distance is larger than the threshold, then the according boundary point is labeled as invalid;

4. Linear basis function model is applied to the new set of valid boundary points whose number is N_2.

The progress is iterative, and could iterate multiple times. Experimental results show that just only one iteration is good enough to refine the boundary curves. Fig.2(f, j) illustrate the refined boundary curves.

5. EXPERIMENTAL RESULTS

Experiments for proposed algorithm are obtained on two available iris databases: CASIA-Iris V3-Interval [11] and IITD v1.0 [12]. The experiments are programmed in Matlab R2007a, progressed on Intel Xeon-Core CPU E5520 (2.27GHz×4). Experimental results are evaluated in follow indexes:

1. Accuracy of segmentation. The iris boundary obtained by the proposed algorithm is compared with the actual iris boundary. If the areas covered by the two boundaries have an

Table 1. The inner and outer iris boundary segmentation accuracy (in %) of our method and Daugman's IDO and AC

	CASIA-Iris V3-Interval			IITD v1.0		
	IDO	AC	Our	IDO	AC	Our
Outer	92.91	93.86	93.97	91.43	92.33	92.59
Inner	86.70	98.76	99.92	83.30	98.48	99.55

Table 2. The time costs (in ms) of our method and Daugman's IDO and AC

	CASIA-Iris V3-Interval			IITD v1.0		
	IDO	AC	Our	IDO	AC	Our
Step 1	162	162	162	142	142	142
Step 2	-	8	0.2	-	8	0.2
Step 3	-	-	3.2	-	-	3.2
Total	162	170	165.4	142	150	145.4

occlusion higher than 95%, then the segmentation is labeled "accurate"; else it is labeled "not accurate". Table 1 shows the segmentation accuracy of the iris inner and outer boundary of our method and Daugman's IDO and AC. From Table 1 we can see the proposed method segments iris with high accuracy, especially the inner boundary.

2. Time cost. The proposed algorithm contains three steps, Table 2 shows the time costs of each step of our method and Daugman's IDO and AC. From Table 2 we can see that the proposed method costs only 3.4 more ms than IDO, which is time economic, and 4.6 less ms than AC.

Roc curves of our method and Daugman's IDO and AC on various databases are shown in Fig.4. To compare performance of different algorithms in iris segmentation module, the same methods are applied to the other modules. Fig.4 shows that the iris recognition system based on the proposed algorithm performs slightly better than that based on Daugman's AC and much better than that based on IDO.

6. CONCLUSIONS

In this paper the iris segmentation problem is regarded as a machine learning one which derives iris boundary curves from coarse iris boundary points, a robust approach of RANSAC is also proposed to remove outliers caused by occlusion. Experimental results show that the proposed method can segment noncircular iris with extremely high accuracy and low computational cost.

7. REFERENCES

[1] K.W. Bowyer, K. Hollingsworth, and P.J. Flynn, "Image understanding for iris biometrics: A survey," *Computer Vision and Image Understanding*, vol. 110, no. 2, pp. 281–307, 2008.

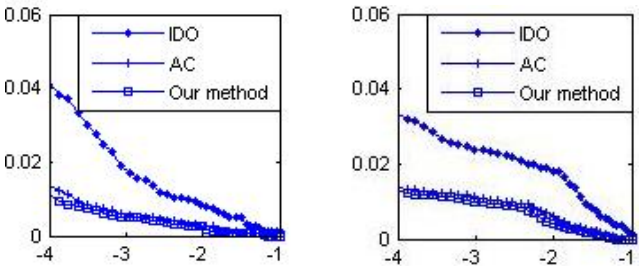

(a) CASIA-Iris V3-Interval (b) IITD v1.0

Fig. 4. ROCs of the proposed method and Daugman's IDO and AC on CASIA-Iris V3-Interval and IITD v1.0.

[2] J.R. Matey, R. Broussard, and L. Kennell, "Iris image segmentation and sub-optimal images," *Image and Vision Computing*, vol. 28, no. 2, pp. 215–222, 2010.

[3] J. G. Daugman, "High confidence visual recognition of persons by a test of statistical independence," *IEEE Trans. On Pattern Analysis and Machine Intelligence*, vol. 15, no. 11, pp. 1148–1161, 1993.

[4] R.P. Wildes, "Iris recognition: an emerging biometric technology," *Proceedings of the IEEE*, vol. 85, no. 9, pp. 1348–1363, 1997.

[5] A. Abhyankar, L. Hornak, and S. Schuckers, "Off-angle iris recognition using bi-orthogonal wavelet network system," in *Fourth IEEE Workshop on Automatic Identification Technologies*, 2005, pp. 239–244.

[6] J. Daugman, "New methods in iris recognition," *IEEE Trans. On Systems, Man, and Cybernetics, Part B: Cybernetics*, vol. 37, no. 5, pp. 1167–1175, 2007.

[7] A. Ross and S. Shah, "Segmenting non-ideal irises using geodesic active contours," in *Special Session on Research at the Biometric Consortium Conference, 2006 Biometrics Symposium*, 2006, pp. 1–6.

[8] M.A. Fischler and R.C. Bolles, "Random sample consensus: a paradigm for model fitting with applications to image analysis and automated cartography," *Commun. ACM*, vol. 24, no. 6, pp. 381–395, 1981.

[9] Karen P. Hollingsworth, Kevin W. Bowyer, and Patrick J. Flynn, "The best bits in an iris code," *IEEE Trans. Pattern Analysis and Machine Intelligence*, vol. 31, no. 6, pp. 964–973, 2009.

[10] C.M. Bishop, Springer, Singapore, 2006.

[11] "Casia," http://www.cbsr.ia.ac.cn/IrisDatabase.htm.

[12] "Iit delhi iris database version 1.0," http://www4.comp.polyu.edu.hk/ csajaykr/IITD/Database_Iris.htm.